

Where Are the Protons in  $\alpha\text{-}[\text{H}_x\text{W}_{12}\text{O}_{40}]^{(8-x)-}$  ( $x = 2\text{--}4$ )?Calvin R. Sprangers, Jason K. Marmon,<sup>†</sup> and Dean C. Duncan\*

Department of Chemistry and Biochemistry, University of Wisconsin—Milwaukee, Milwaukee, Wisconsin 53201

Received July 22, 2006

The equilibria and speciation of the proton cryptate polyoxometalate  $\alpha\text{-}[(\text{H}_2)\text{W}_{12}\text{O}_{40}]^{6-}$  (**1**) were examined by NMR following the phase-transfer cation metathesis of aqueous  $\text{Na}_6\mathbf{1}$  with  $\text{Q}^+\text{Br}^-/\text{CH}_2\text{Cl}_2$ , leading to the isolation of the  $(n\text{-Bu})_4\text{N}^+$  ( $\text{Q}^+$ ) salts  $\text{Q}_6\mathbf{1}$  and  $\alpha\text{-Q}_5\text{-}[(\text{H}_3)\text{W}_{12}\text{O}_{40}]$  (**Q52**). Several groups report salts of the protonated anions  $\text{H}_x\mathbf{1}$  ( $x = 1$  and  $2$ ) with no consensus on proton numbers or locations. Reported herein, a combination of  $^1\text{H}$  and  $^{183}\text{W}$  NMR evidence, elemental analysis, acid titration measurements, and H/D isotopomer assignments establishes that in nonaqueous media the internal cryptand cavity of **1** reversibly accommodates only one more proton to form **2**. Because an external proton must transfer across the close-packed tungsten oxide surface of **1**, which should constitute a substantial activation barrier, it is significant that the transformation is instantaneous by  $^1\text{H}$  NMR (1 equiv of HBr in  $\text{CH}_3\text{CN}$ ), whereas the reverse process is slow ( $t_{1/2} \sim 17.4$  h; 1 equiv of  $\text{Q}^+\text{OH}^-$ ).

Proton cryptate complexes, particularly those derived from metal–oxygen frameworks, are rare, with most examples originating from the protonation of azamacrocycles.<sup>1</sup> The  $\alpha$  isomer of the metatungstate anion,  $\alpha\text{-}[(\text{H}_2)\text{W}_{12}\text{O}_{40}]^{6-}$  (**1**), represents a prototypical example of a wholly inorganic proton cryptate with two protons “entombed” within the solvent-inaccessible interior of this polyoxometalate (POM) complex (Figure 1).<sup>2–4</sup> The proton cryptate nature of **1** is underscored by numerous studies of **1** in aqueous solutions that reveal no evidence for exchange of its internal protons with water or for its further protonation.<sup>5–8</sup> Under nonaqueous conditions, however, a triprotonated species is reported by Fuchs and Flindt as a tri-*n*-butylammonium salt and the



**Figure 1.** Polyhedral representation of **1**, the  $\alpha$ -Keggin structure, consisting of four sets of three edge-shared  $\text{WO}_6$  octahedra or triads linked together by shared corners. This  $\text{W}\text{--}\text{O}$  framework encloses a central cryptand cavity defined by four internal  $\mu_3$ -bridging O atoms, one from each triad, arranged in a tetrahedron about the anion center with overall  $T_d$  symmetry for the formal  $\alpha\text{-}[\text{W}_{12}\text{O}_{40}]^{8-}$  unit. The two protons (blue) are coordinated to and rapidly exchange among the four equivalent internal O atoms, thus preserving the  $T_d$  symmetry of the anion on the NMR time scale, as is consistent with the  $^1\text{H}$ ,  $^{17}\text{O}$ , and  $^{183}\text{W}$  NMR spectra of **1** in an aqueous solution.<sup>6,10</sup>

anion formulated as  $\alpha\text{-}[(\text{H}_3)\text{W}_{12}\text{O}_{40}]^{5-}$  (**2**) with all three protons assigned to the internal cryptand cavity.<sup>9</sup> However, this view has not been met with wide acceptance, presumably because of the well-documented behavior of **1** in water. Indeed, assignment of the third proton as an external countercation with the anion formulated as  $\alpha\text{-H}[(\text{H}_2)\text{W}_{12}\text{O}_{40}]^{5-}$  (**H1**) is favored both in the review literature<sup>11</sup> and in a recent study by Boskovic et al., who report the tetra-*n*-butylammonium ( $\text{Q}^+$ ) salt,  $\text{Q}_5\text{H1}$ .<sup>12</sup> Furthermore, a tetra-protonated species is reported by Himeno et al. as  $\alpha\text{-}[(\text{H}_4)\text{W}_{12}\text{O}_{40}]^{4-}$  with all four protons assigned to the internal

\* To whom correspondence should be addressed. E-mail: dcduncan@uwm.edu.

<sup>†</sup> Current address: Department of Chemistry, Beloit College, Beloit, WI 53511.

- (1) (a) Morehouse, P.; Hossain, M. A.; Llinares, J. M.; Powell, D.; Bowman-James, K. *Inorg. Chem.* **2003**, *42* (25), 8131–8133. (b) Miyahara, Y.; Tanaka, Y.; Amimoto, K.; Akazawa, T.; Sakuragi, T.; Kobayashi, H.; Kubota, K.; Suenaga, M.; Koyama, H.; Inazu, T. *Angew. Chem., Int. Ed.* **1999**, *38* (7), 956–959. (c) Kuldova, K.; Corval, A.; Trommsdorff, H. P.; Lehn, J. M. *J. Phys. Chem. A* **1997**, *101* (37), 6850–6854.
- (2) Freedman, M. L. *J. Am. Chem. Soc.* **1959**, *81* (15), 3834–3839.
- (3) Pope, M. T.; Varga, G. M., Jr. *Chem. Commun.* **1966**, *18*, 653–654.
- (4) Asami, M.; Ichida, H.; Sasaki, Y. *Acta Crystallogr., Sect. C* **1984**, *40*, 35–37.

- (5) (a) Souchay, P.; Boyer, M.; Chaveau, F. K. *Tek. Hoegsk. Handl.* **1972**, *259*. (b) Launay, J. P. *J. Inorg. Nucl. Chem.* **1976**, *38*, 807–816. (c) Launay, J. P.; Boyer, M.; Chauveau, F. *J. Inorg. Nucl. Chem.* **1976**, *38*, 243–247.
- (6) Hastings, J. J.; Howarth, O. W. *J. Chem. Soc., Dalton Trans.* **1992**, *2*, 209–215.
- (7) Smith, B. J.; Patrick, V. A. *Aust. J. Chem.* **2000**, *53*, 965–970.
- (8) Niu, J. Y.; Zhao, J.; Wang, J. P.; Bo, Y. *J. Coord. Chem.* **2004**, *57* (11), 935–946.
- (9) Fuchs, J.; Flindt, E.-P. *Z. Naturforsch.* **1979**, *34b*, 412–422.
- (10)  $^{183}\text{W}$  (one peak: 12 W),  $^{17}\text{O}$  (four peaks: 12 O, terminal; 12 O,  $\mu_2$ -corner-shared; 12 O,  $\mu_2$ -edge-shared; 4 O  $\mu_3$ -central cavity), and  $^1\text{H}$  (one peak: 2 H).
- (11) (a) Pope, M. T. *Heteropoly and Isopoly Oxometalates*; Springer-Verlag: Berlin, 1983. (b) Pope, M. T. Isopolyanions and Heteropolyanions. In *Comprehensive Coordination Chemistry*; Wilkinson, G., Gillard, R. D., Eds.; Pergamon: New York, 1987; pp 1023–1058. (c) Pope, M. T. Polyoxo Anions: Synthesis and Structure. In *Comprehensive Coordination Chemistry II: From Biology to Nanotechnology. Transition Metal Groups 3–6*; Wedd, A. G., Ed.; Elsevier Science: New York, 2004; Vol. 4, pp 635–678.
- (12) Boskovic, C.; Sadek, M.; Brownlee, R. T. C.; Bond, A. M.; Wedd, A. G. *J. Chem. Soc., Dalton Trans.* **2001**, *2*, 187–196.

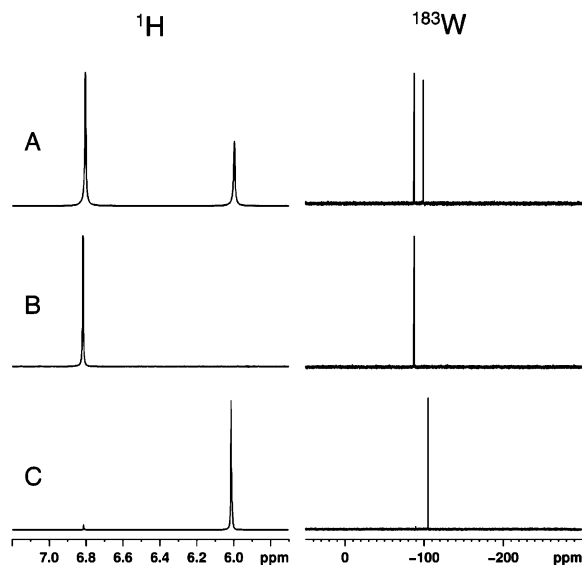


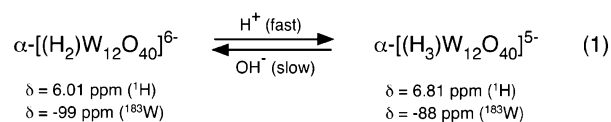
**Figure 2.**  $^1\text{H}$  (500 MHz) and  $^{183}\text{W}$  (20.8 MHz) NMR spectra of (A) an equilibrated  $\text{Q}^+$  extract of  $\text{Na}_6\text{I}$  (aqueous-phase initial pH = 5.17) reconstituted in  $\text{CD}_3\text{CN}$ , (B) the addition of  $\text{HBr}$  (0.0802 M in  $\text{CH}_3\text{CN}$ , 1 equiv) to the extract in part A, and (C) the addition of  $\text{Q}^+\text{OH}^-$  (1 M in  $\text{MeOH}$ , 1.3 equiv) to an anhydrous  $\text{CH}_3\text{CN}$  solution of  $\text{Q}_5\text{Z}$  (vide infra) with field lock provided by  $\text{CD}_3\text{CN}$  within a coaxial insert.  $^1\text{H}$  and  $^{183}\text{W}$  NMR chemical shifts are reported relative to tetramethylsilane in  $\text{CD}_3\text{CN}$  and 2 M  $\text{Na}_2\text{WO}_4$  in  $\text{D}_2\text{O}$ .

cavity.<sup>13</sup> Because these reports indicate no consensus on the number and location of added protons to  $\alpha$ -metatungstate, these issues require reassessment.

We report herein a reexamination of metatungstate equilibria and speciation following the phase-transfer cation metathesis of aqueous  $\text{Na}_6\text{I}$  using  $\text{Q}^+\text{Br}^-$  in  $\text{CH}_2\text{Cl}_2$ , as is first reported by Boskovic et al for the preparation of  $\text{Q}_5\text{HI}$ .<sup>12</sup> Two interconverting species are identified and assigned unambiguously as **1** and **2**, wherein **2** can be protonated further only to **H2**, thereby resolving confusion on metatungstate protonation in nonaqueous media. Of particular significance is the observation of fast kinetics for the formation of **2** from **1**. Because an external proton must transfer across a close-packed surface of kinetically inert  $\text{W}-\text{O}$  bonds, which in other metal oxides normally constitutes a substantial activation barrier,<sup>14</sup> such a fast proton transfer is unprecedented as far as we are aware and challenges our understanding of proton transfer and conductivity in metal oxides. Detailed studies of the kinetics and mechanism of proton transfer are in progress.

Phase transfer of aqueous  $\text{Na}_6\text{I}$  (20 mM; initial pH = 3, 5, 6, and 8) into a  $\text{CH}_2\text{Cl}_2$  solution of  $\text{Q}^+\text{Br}^-$  (6 equiv, 200 mM) by cation metathesis does not lead to the clean formation of  $\text{Q}_6\text{I}$ . Instead, NMR examination of these  $\text{Q}^+$  extracts either directly in  $\text{CH}_2\text{Cl}_2$  (after drying over  $\text{MgSO}_4$ ) or by first removing the solvent under vacuum followed by reconstitution in acetonitrile- $d_3$  ( $\text{CD}_3\text{CN}$ ) reveals two resonances each in both  $^1\text{H}$  and  $^{183}\text{W}$  NMR spectra (Figure 2A). Boskovic et al. report NMR data for *isolated*  $\text{Q}_5\text{HI}$  ( $^1\text{H}$ ,  $\delta$

= 6.80 ppm;  $^{183}\text{W}$ ,  $\delta$  = -91.3 ppm) that are similar to those in Figure 2A ( $^1\text{H}$ ,  $\delta$  = 6.81 ppm;  $^{183}\text{W}$ ,  $\delta$  = -87.6 ppm). The other pair of resonances ( $^1\text{H}$ ,  $\delta$  = 6.01 ppm;  $^{183}\text{W}$ ,  $\delta$  = -99 ppm) has not been reported.<sup>12</sup> All other peaks in the  $^1\text{H}$  NMR spectra originate from  $\text{Q}^+$  counterions and solvent, and all chemical shifts are independent of the aqueous-phase initial pH. However, the relative peak integrals in both  $^1\text{H}$  and  $^{183}\text{W}$  NMR spectra slowly change, with equilibration reached usually within 24 h. During this period, the sum of the two  $^1\text{H}$  NMR peak integrals does not change relative to those from the  $\text{Q}^+$  counterion, which serves as an internal standard and establishes the slow approach to equilibrium as an interconversion between two proton populations. Similarly, the relative changes in  $^{183}\text{W}$  NMR peak integrals also are consistent with an interconversion between two W populations. Furthermore, as the initial pH of the aqueous phase increases from 3, 5, 6, to 8, the  $^1\text{H}$  and  $^{183}\text{W}$  NMR peak integrals of the equilibrated  $\text{Q}^+$  extracts also increase for the resonance pair ( $^1\text{H}$ ,  $\delta$  = 6.01 ppm;  $^{183}\text{W}$ ,  $\delta$  = -99 ppm), with concomitant decreases for the pair ( $^1\text{H}$ ,  $\delta$  = 6.81 ppm;  $^{183}\text{W}$ ,  $\delta$  = -87.6 ppm) assigned previously to **H1**.<sup>12</sup> This behavior is derived from  $\text{OH}^-$  extracted into  $\text{CH}_2\text{Cl}_2$  because it mirrors that observed upon the addition of  $\text{Q}^+\text{OH}^-$  directly to an equilibrated  $\text{Q}^+$  extract solution, including the slow approach to equilibrium (Figure 2C), whereas the opposite and instantaneous peak transformation behavior is observed upon the addition of hydrobromic acid (Figure 2B). Taken together, these data are consistent with the formation and reversible interconversion of two POMs of the general formula  $\alpha\text{-}[(\text{H}_x)\text{W}_{12}\text{O}_{40}]^{(8-x)-}$  that differ only in the number of internal protons,  $x$ , and equilibrate either rapidly in the presence of suitable Brønsted acids or slowly with bases, while maintaining effective  $T_d$  symmetry on the NMR time scale (eq 1). Although a fast exchange of an external proton



between POM surface O atoms and residual water is consistent with the NMR data,<sup>12</sup> it is not consistent with the slow rate of anion deprotonation, which instead is typical of proton cryptate behavior.

The number of protons assigned to each species shown in eq 1 was determined from three independent measurements. First, an equilibrated  $\text{Q}^+$  extract in  $\text{CH}_3\text{CN}$  was titrated with a standardized hydrobromic acid solution (0.0802 M), and  $^1\text{H}$  NMR peak integrals were measured at equilibrium relative to a naphthalene internal standard (0.1077 M) in  $\text{CD}_3\text{CN}$  housed within a coaxial insert tube (Figure 3). This experiment allowed for field locking while avoiding potential hydrogen/deuterium (H/D) exchange from interference with the measurements of the  $\text{H}^+$  concentration associated with each POM. In a model of two interconverting species,  $[(\text{H}_x)\text{W}_{12}\text{O}_{40}]^{(8-x)-}$  and  $[(\text{H}_{x+n})\text{W}_{12}\text{O}_{40}]^{(8-x-n)-}$ , that differ by  $n$  protons, the theoretical slopes in the plots of moles of  $\text{H}^+$  within each POM versus moles of  $\text{HBr}$  added are  $-x$  for  $[(\text{H}_x)\text{W}_{12}\text{O}_{40}]^{(8-x)-}$  at  $\delta$  = 6.01 ppm and  $x + n$  for

(13) Himeno, S.; Yoshihara, M.; Maekawa, M. *Inorg. Chim. Acta* **2000**, 298, 165–171.

(14) (a) Rao, C. N. R.; Raveau, B. *Transition Metal Oxides*; John Wiley & Sons: New York, 1998. (b) Smyth, D. M. *The Defect Chemistry of Metal Oxides*; Oxford University Press: New York, 2000.

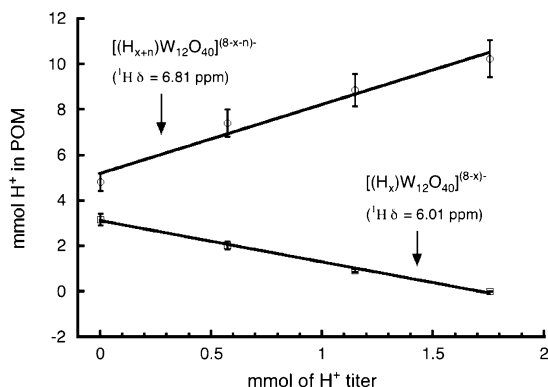


**Figure 3.** Titration of an equilibrated  $Q^+$  extract of  $Na_6\mathbf{1}$  with standardized hydrobromic acid (0.0802 M) in  $CH_3CN$ . Integration of the  $^1H$  NMR peaks relative to a naphthalene internal standard (0.1077 M in  $CD_3CN$ ) housed within a coaxial insert tube enabled the number of millimoles of  $H^+$  within each POM to be determined. The titration plots were fit to linear functions:  $\alpha\text{-}[(H_x)W_{12}O_{40}]^{(8-x)-}$ , slope =  $-x = -1.82$ , intercept = 3.12,  $R^2 = 0.996$ ;  $\alpha\text{-}[(H_{x+n})W_{12}O_{40}]^{(8-x-n)-}$ , slope =  $x + n = 3.03$ , intercept = 5.2,  $R^2 = 0.970$ .

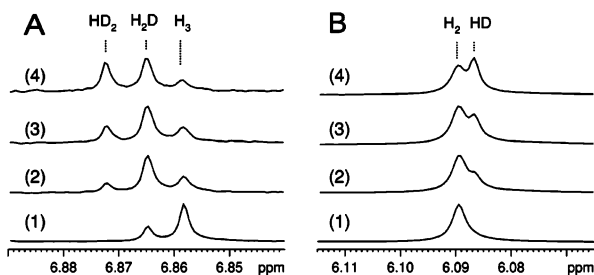


**Figure 4.** Temporal evolution in the  $^1H$  (500 MHz) NMR spectra of the isotopomers  $[(H_{3-x}D_x)W_{12}O_{40}]^{5-}$  (A) and  $[(H_{2-x}D_x)W_{12}O_{40}]^{6-}$  (B) formed by heating a solution of  $Q_5\mathbf{2}$  (89 mM) in  $CD_3CN$  with  $Q^+OH^-$  (1.3 equiv, 1 M in methanol) at  $60^\circ C$  within the NMR probe for (1) 35 min, (2) 140 min, (3) 245 min, and (4) 470 min.

$[(H_{x+n})W_{12}O_{40}]^{(8-x-n)-}$  at  $\delta = 6.81$  ppm, respectively. Equating these with the measured slopes in Figure 3 gives  $x = 1.8$  and  $x + n = 3.0$ , indicating that the transformation is monoprotic and that the experimental average value of  $x$  is 1.9, which unambiguously establishes the identities of the two POMs in solution as the diprotonated complex **1** and an internally triprotonated species **2** whose elemental constitution is otherwise in agreement with that of Boskovic et al.<sup>12</sup> No further peak transformations were observed up to 1 week after the addition of acid. Second, both **1** and **2** were isolated and purified as  $Q^+$  salts, giving elemental analyses, cyclic voltammograms, and  $^1H$  and  $^{183}W$  NMR data that are consistent with the formulations  $Q_6\mathbf{1}$  and  $Q_5\mathbf{2}$  (see Figure 2 and the Supporting Information). Third,  $^1H$  NMR monitoring at  $60^\circ C$  of the deprotonation of  $Q_5\mathbf{2}$  (89 mM) in  $CD_3CN$  by  $Q^+OH^-$  (1 equiv, 1 M in methanol) to form **1** also revealed H/D isotope exchange between  $OH^-$  and  $CD_3CN$  followed by the incorporation of deuterium within both POMs (Figure 4). The spectra show the following evolutions: **2** ( $\delta = 6.858$  ppm)  $\rightarrow [(H_2D)W_{12}O_{40}]^{5-}$  ( $\delta = 6.865$  ppm)  $\rightarrow [(HD_2)W_{12}O_{40}]^{5-}$  ( $\delta = 6.872$  ppm) and **1** ( $\delta = 6.090$  ppm)  $\rightarrow [(HD)W_{12}O_{40}]^{6-}$  ( $\delta = 6.087$  ppm). A  $^2H$  NMR spectrum confirmed deuterium enrichment in both **1** and **2**.

Additional evidence was obtained from a single kinetics measurement of the deprotonation of  $Q_5\mathbf{2}$  by  $Q^+OH^-$  (Figure S1 in the Supporting Information). Although the data are

insufficient to distinguish between first- and second-order kinetics, they were fit satisfactorily to a first-order model for the sake of comparison with observed rate constants and amplitudes for the decay of **2** [ $k = (1.11 \pm 0.06) \times 10^{-5} s^{-1}$ ;  $A_0 = 3.1 \pm 0.1$ ] and the rise of **1** [ $k = (1.13 \pm 0.1) \times 10^{-5} s^{-1}$ ;  $A_\infty = 2.0 \pm 0.1$ ], as is consistent with the equilibrium and protonation assignments in eq 1 and indicates a substantial kinetic barrier for the deprotonation of **2**. The kinetics for protonation of **1** are too rapid for  $^1H$  NMR measurements.

The basicity of  $Q_6\mathbf{1}$  in  $CH_3CN$  is similar to that of triethylamine ( $pK_a \sim 18.8$ )<sup>15</sup> because significant protonation of **1** to **2** occurs in the presence of 1 equiv of triethylammonium chloride. However, further *internal* protonation of **2** with 1 equiv of either hydrobromic or *p*-toluenesulfonic acid ( $pK_a \sim -9$  and  $-2$ , respectively) fails; the  $^1H$  NMR resonance at  $\delta = 6.81$  ppm shifts downfield to  $\delta = 6.89$  ppm with no change in the relative integrated intensity. Therefore, the tetraprotonated species reported by Himeno et al. is reassigned as **H2** with an *external* proton counterion.<sup>13,16</sup>

Cyclic voltammograms of  $Q_6\mathbf{1}$  and  $Q_5\mathbf{2}$  were recorded in  $CH_3CN$  with  $Q^+[PF_6]^-$  as the supporting electrolyte using a glassy carbon working electrode (Figure S2 in the Supporting Information). For  $Q_6\mathbf{1}$ , a single quasi-reversible reduction takes place at  $E_{1/2} = -1.934$  V vs  $Ag/AgNO_3$  (peak–peak separation,  $\Delta E_p = 0.090$  V), whereas  $Q_5\mathbf{2}$  exhibits two one-electron processes at  $-1.486$  ( $\Delta E_p = 0.068$  V) and  $-1.970$  V ( $\Delta E_p = 0.075$  V). The ferrocenium/ferrocene redox couple under these conditions is  $E_{1/2} = +0.06$  V. These data reflect the known strong influence of the anion charge on the POM reduction potential, where the 450-mV separation between the first reduction potentials of  $Q_6\mathbf{1}$  and  $Q_5\mathbf{2}$  is typical of  $\alpha$ -Keggin POMs in nonaqueous solvents, as is the 36-mV separation in reduction potentials between the isocharged species  $\alpha\text{-}[(H_3)W_{12}O_{40}]^{6-}$  and **1**.<sup>17,18</sup> Measurements of the protonation equilibria, associated reaction kinetics, internal proton dynamics, and mixed-valence structure in nonaqueous solutions of **1** and **2** are in progress.<sup>19</sup>

**Acknowledgment.** J.K.M. thanks the Ronald E. McNair Program for an undergraduate summer research internship, and the University of Wisconsin system is gratefully acknowledged for financial support.

**Supporting Information Available:** Synthesis, analytical data, and cyclic voltammograms of  $Q_6\mathbf{1}$  and  $Q_5\mathbf{2}$  along with preliminary kinetics data on the deprotonation of  $Q_5\mathbf{2}$ . This material is available free of charge via the Internet at <http://pubs.acs.org>.

IC061370C

- (15) Kaljurand, I.; Kütt, A.; Sooväli, L.; Rodima, T.; Mäemets, V.; Leito, I.; Koppel, I. A. *J. Org. Chem.* **2005**, *70*, 1019–1028.
- (16) NMR data reported in ref 13 are consistent with rapid exchange between a fourth proton on the POM exterior and water observed at  $\delta = 2.1$  ppm, which was misassigned to the cryptate protons.
- (17) (a) Pope, M. T.; Varga, G. M., Jr. *Inorg. Chem.* **1966**, *5*, 1249–1254. (b) Altenau, J. J.; Pope, M. T.; Prado, R. A.; So, H. *Inorg. Chem.* **1975**, *14* (2), 417–421.
- (18) Maeda, K.; Katano, H.; Osakai, T.; Himeno, S.; Saito, A. *J. Electroanal. Chem.* **1995**, *389*, 167–173.
- (19) A reviewer noted that the  $^{183}W$  NMR spectra (Figure 2) also require that the rate of  $^1H$  exchange between **1** and **2** must be  $k_{ex} \ll 237 s^{-1}$ .